JOURNAL OF PHYSICAL ORGANIC CHEMISTRY
J. Phys. Org. Chem. 2002; **15:** 647–659
Published online in Wiley InterScience (www.interscience.wiley.com). DOI: 10.1002/poc.528

Study of inclusion complexes of acridine with β- and (2,6-di-*O*-methyl)-β-cyclodextrin by use of solubility diagrams and NMR spectroscopy

Isabelle Correia,[1] Nabil Bezzenine,[1] Nello Ronzani,[1] Nicole Platzer,[2] Jean-Claude Beloeil[2] and Bich-Thuy Doan[2]*

[1]Laboratoire de Chimie Structurale Organique et Biologique, UPMC Paris 6, Bat. F, BP 45, 4 place Jussieu, 75252 Paris Cedex 05, France
[2]Laboratoire de RMN Biologique, ICSN, CNRS, Avenue de la Terrasse 91198 Gif-sur-Yvette Cedex, France

Received 30 December 2001; revised 30 March 2002; accepted 16 April 2002

epoc ABSTRACT: Previous molecular modeling studies, in our laboratory, have shown that some esters of type $RCOO(CH_2)_nC_5H_5N^+Cl^-$ are potentially active against Alzheimer's disease. We have also demonstrated that acridine, which has strong anticholinesterase activity appears to be a suitable R substituent. The main obstacle to the possible pharmaceutical application of these compounds is their limited solubility in water, which is due to the poor aqueous solubility of acridine itself (0.26 mM). Inclusion complexation with cyclodextrins may overcome this problem. Solubility diagrams and NMR spectroscopy were used to study the inclusion of acridine (Acr) within β-cyclodextrin (βCD) and heptakis(2,6-di-*O*-methyl)cyclomaltoheptose (DMβCD). A 1:1 complex was formed for the Acr–βCD system and both 1:1 and 2:1 complexes for the Acr–DMβCD system (apparent K_a 215 ± 20 and 1150 ± 100 M^{-1}, respectively). Data from ^1H NMR studies corrected the assignment of the acridine H1, H8 and H4, H5 protons in D_2O, which have been erroneously assigned in previous publications. ^1H spin–lattice relaxation times T_1 measured with selective, non-selective and null inversion characterize the dynamics of the inclusion complexes. Geometric features of the host–guest inclusion complexes were inferred from intermolecular dipolar interactions obtained by 2D adiabatic off-resonance ROESY experiments. A more detailed picture of the structure of the inclusion complexes was obtained by combining NMR structural data and molecular modeling (docking, dynamics under NMR constraints and energy calculations). Copyright © 2002 John Wiley & Sons, Ltd.
Additional material for this paper is available from the epoc website at http://www.wiley.com/epoc

KEYWORDS: NMR; solubility diagrams; β-cyclodextrins; inclusion complexes; acridine; dynamics; molecular modeling

INTRODUCTION

Some 2,5-disubstituted tetrahydrofuran derivatives **A** (Fig. 1) which inhibit platelet aggregation (PAF antagonists) are also potential inhibitors of the cholinesterases, the fundamental enzymes in the propagation of the nervous impulses. These compounds are promising candidates for the treatment of Alzheimer's disease.[1] Introduction of a long aliphatic chain ($n = 6$) bearing a carbamate group and a pyridinium moiety appears to be required for both platelet aggregation and acetylcholinesterase inhibition. From molecular modeling of potential cholinesterase inhibitors, previous laboratory studies have shown that some esters of type **B** $RCOO(CH_2)_nC_5H_5N^+Cl^-$ are competitive inhibitors of cholinesterases (e.g. R = cyclohexyl, phenyl, biphenyl, 1-naphthyl), and have anticholinesterase activity ($IC_{50} \approx 10^{-7}$, $n = 6$) similar to that of physostigmine. The current study concerns acridine (Acr), a potential R substituent, which itself exhibits significant anticholinesterase activity.[2] Acridine has poor solubility in water (2.6×10^{-4} M), but it is a basic motif found in many anticholinesterase compounds. The derivatives of acridine or dibenzopyridine are principally antiseptic, antimalarial or cholinergic.[3] The main obstacle to the eventual pharmaceutical application of $AcrCOO(CH_2)_nC_5H_5N^+Cl^-$ derivatives is their limited water solubility, due to the low aqueous solubility of acridine. Furthermore, some derivatives of acridine which do have pharmacological activity also display adverse side-effects.

During the last few years, several medicinal substances have been successfully complexed by cyclodextrins (CDs).[4] This has increased the stability and hydrosolubility of the substance, and modified the pharmacokinetics of the resulting drugs, with a subsequent reduction in adverse effects.[5] Several drugs from the following categories have already been included within cyclodex-

**Correspondence to:* B.-T. Doan, Laboratoire de RMN Biologique, ICSN, CNRS, Avenue de la Terrasse, 91198 Gif-sur-Yvette Cedex, France.
E-mail: doan@icsn.cnrs-gif.fr

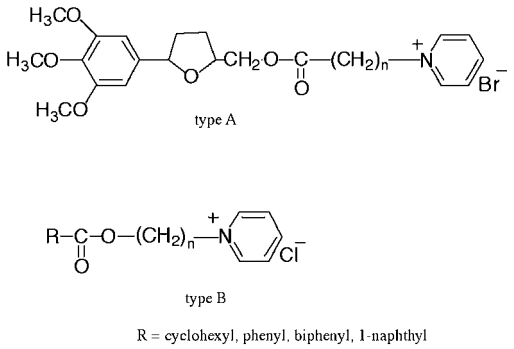

Figure 1. Potential acetylcholinesterase inhibitors

trins:[6] anti-inflammatories, barbiturates, anti-epileptics and anti-cancerous drugs. These new combinations have recently been marketed in Europe, the USA and Japan. For an example, a nonsteroidal anti-inflammatory molecule, Brexin, has been on sale in France since 1993 (Piroxicam–β-cyclodextrin association). βCD is used and marketed in a series of drugs such as prostaglandin, benexate, dexamethazone, etc. It has been found that cyclodextrins significantly increase the water solubility of hydrocortisone and progesterone molecules.

The study of the acridine–CD complexes is the first approach used to evaluate the biosolubility of our potential anticholinesterase and hydrophobic **B** compounds (Fig. 2). βCD was compared with DMβCD, which is more soluble.[7] We used solubility diagrams and NMR spectroscopy to investigate the complexation of acridine by cyclodextrins. However, the first method provides only indirect qualitative information about the inclusion and geometry of cyclodextrin complexes. NMR spectroscopy has become the main method for elucidating the structure, kinetics and dynamics of supramolecular host–guest complexes in the dissolved state.[8] Because of the low solubility of acridine in water, we used ^{1}H NMR in these studies (changes in the chemical shift of acridine protons, selective ^{1}H T_1 measurements, nuclear Overhauser effect). Finally, more quantitative structural data can be obtained by the combined use of NOE data and molecular dynamics and molecular mechanics calculations.

EXPERIMENTAL

Solubility diagrams. The solubility isotherms of the Acr–CD systems were obtained at 25 °C using the technique proposed by Higuchi and Connors.[9] The solubilized Acr was quantified by UV spectroscopy with a Philips spectrophotometer. UV absorption was measured on the 356 nm band (π–π* transition) with 0.2 cm lightpath quartz cells. It was checked that the molar absorption coefficient of Acr does not change significantly upon inclusion ($\varepsilon = 9200\ \text{M}^{-1}\,\text{cm}^{-1}$). The phase solubility diagrams were constructed by plotting the molar solubility of acridine as a function of the total molar concentration of CD added.

NMR spectroscopy. 1D ^{1}H (NOE difference experiments, NMR titrations) and 2D COSY, LR-COSY, HSQC, HMBC NMR spectra were performed on Bruker AM-500 (500.13 MHz) and DMX-500 (500.11 MHz)

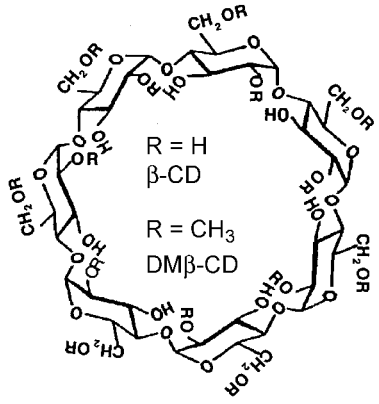

Cyclodextrins

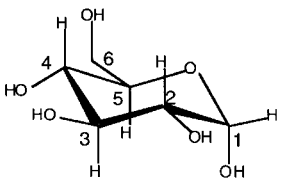

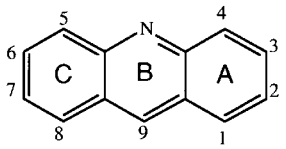

Acridine

Figure 2. Structures of the molecules investigated

spectrometers with a 5 mm (Z-gradient for DMX) reverse probe at 298, 303 or 310 K. ^{1}H spin–lattice relaxation time (^{1}H T_1) experiments and adiabatic off-resonance ROESY spectra were recorded with an 8 mm ^{1}H Z-gradient probe.

^{1}H NMR experiments were carried out in D_2O solution with the residual HOD signal as internal standard (4.75 ppm at 298 K, 4.70 ppm at 303 K and 4.63 ppm at 310 K), and in methanol solution (CD_3OD) with residual solvent signal resonance at 3.31 ppm at 298 K.

COSY and LR-COSY[10] (with an optimized long-range delay equal to 140 ms) were acquired at 298 K using 160 t_1 increments with 2K data points and 320 scans each. Partial suppression of the residual HDO signal was accomplished by a presaturation during the 1.5 s relaxation delay. The data were processed with a non-shifted sine-bell window in both dimensions.

The phase-sensitive gradient-selected HSQC[11] and gradient-selected HMBC[12] (delay = 70 ms corresponding to $^3J_{C-H} = 7$ Hz was used) experiments were recorded at 303 K. These experiments were acquired using 256 t_1 increments with 2K data points and 64 scans (HSQC) or 96 scans (HMBC). Two zero-fillings were applied in the t_1 dimension and a $\pi/3$ shifted squared sine-bell function was used in both dimensions.

An adiabatic off-resonance ROESY experiment has been proposed in order to overcome the inherent drawbacks of conventional ROESY.[13] The HOHAHA coherence transfer was suppressed and the offset dependence was minimized for quantification purposes. The spin-locking carrier frequency was shifted by +5.5 kHz from the center of the spectrum. The improved version of the initial pulse sequence was used.[14] 2D ROESY spectra were obtained using a spectral width of 5 kHz, with 2K complex points in f_2, 256 t_1 values, 320 scans per incremented t_1 and a relaxation delay of 2 s. The angle between static and effective field was equal to 54.7°. A trapezoidal adiabatic spin lock with an average mixing time of 300 ms was applied with 0.25% random variation. The spin-lock field strength was ~8 kHz. After zero-filling to a 2 K × 1 K matrix, π/n shifted sine-bell functions were applied in both dimensions (n = 2, 4, 16 or 32).

Non-selective ^{1}H T_1 values were measured using the inversion–recovery method. Thirty-two scans were acquired into 32K data points with a spectral width of 5 kHz and a relaxation delay of 62 s for free acridine and 30 s for acridine–cyclodextrin mixtures. The interval between the 180° and 90° pulses was varied in the range 0.1–62 s for the free acridine and 0.05–30 s for complexed acridine with βCD or DMβCD. Selective experiments were carried out with the null inversion sequence[15] using a 70 ms I-Burp selective pulse. The relaxation rates were calculated by a direct least-squares fitting to a three-parameter exponential equation which is available in the NMR spectrometer Xwinmr program. For the last two experiments a WATERGATE sequence was included to suppress the solvent peak

Molecular modeling. Classical molecular mechanics and restrained dynamics simulation protocols were used to explore the conformational space and search for a stable conformation. Calculations were computed on an SGI Indigo 2 workstation using the SYBYL software package (version 6.5, Tripos, St. Louis, MO, USA). The interproton distance constraints were derived from the quantitative ROE data recorded at the mixing time, t_m = 400 ms, by integrating the volume of the ROESY spectra cross peaks. Build-up curves showed that the values had been taken from the linear portion. The distance between the *ortho* H1–H2 protons of acridine was set to 1.98 Å as a calibration distance. Further constraints on the cyclodextrin, i.e. the angles between four glycoside oxygen atoms (0°) and angles between three consecutive glycoside oxygen atoms (125°), were added to keep the global geometry of the macrocycle.[16] The NOE force constants were kept at 2 kcal mol^{-1} Å^{-2} for the angles constraints and to 50 kcal mol^{-1} Å^{-2} for the distance range constraints. Gasteiger–Hückel charges were applied to the complex. Docking, followed by a minimization using Tripos force field to refine the covalent geometry (200 steps steepest descent, 200 steps conjugate gradient), were computed. The structures were refined by a molecular dynamics stage under the following constraints: 1.5 ps heating from 200 to 1000 K, 10 ps equilibration at 1000 K, 6 ps cooling to 300 K and 10 ps equilibration at 300 K, and a final minimization (250 steps steepest descent, 250 steps conjugate gradient, 500 steps Powell method) were used to search for a stable conformation of the complex. Twenty energetically stable conformations were selected out of 100 total simulated RMD structures with minimum violations of distances and angles.

Sample preparation. Acridine and β-cyclodextrin were purchased from Aldrich (France). Highly isomerically pure heptakis(2,6-di-*O*-methyl)-β-CD was purchased from CTD (Florida, USA). The samples were prepared with deuterated water (99.8%, purchased from CEA, France). The cyclodextrins were used without further purification.

For the preparation of acridine–βCD or DMβCD solutions for solubility diagrams, a saturated acridine solution was prepared with 2 mg of acridine and 3 ml of water. Increasing amounts of cyclodextrin were added to the acridine solution in the presence of an excess of solid acridine. The samples were mixed at constant temperature (25 °C) until a steady state was reached (15 h; preliminary experiments showed that this time was long enough). After centrifugation, the total concentration of drug was determined in the supernatants.

For the preparation of acridine–βCD or DMβCD solutions for NMR measurements, the ^{1}H NMR experiments involved titration of a 0.2 mM solution of acridine after successive additions of solid cyclodextrin until there was no significant change in the chemical shift values

between successive NMR spectra. The concentrations of the cyclodextrins ranged from 0.5 to 10 mM in increments of 1 mM for βCD and of 0.5 mM for DMβCD. The spectra were recorded after 15 h under stirring at 303 K.

For the studies of complexes by ^{1}H T_1 measurements, 1 mg of solid acridine was added to 3 ml of a 5 mM solution of cyclodextrin in D_2O. The mixture was kept at 303 K under stirring for 15 h before measurements. The total concentration of soluble acridine determined by UV spectrophotometry was 0.56 and 1.40 mM in the presence of βCD and DMβCD, respectively. T_1 measurements were carried out at 303 K.

Similar processes were used for the ROESY experiments recorded at 310 K for the Acr–βCD mixture and at 303 K for the Acr–DMβCD mixture. The solutions were deoxygenated by bubbling argon gas through them.

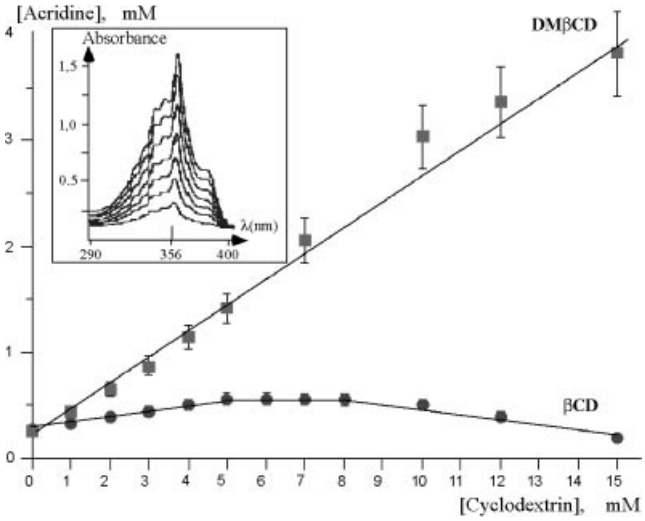

Figure 3. Phase solubility diagrams for acridine in presence of βCD and DMβCD at 298 K. Inset: absorbance increase at 356 nm upon addition of DMβCD

RESULTS

Determination of the apparent equilibrium constants by solubility measurements

The phase solubility diagrams corresponding to the Acr–βCD and Acr–DMβCD systems are shown in Fig. 3. Acridine showed a B_S-type solubility curve, as defined by Higuchi and Connors[9], with βCD, indicating the formation of a poorly soluble 1:1 inclusion complex. As expected for this type of solubility diagram when βCD is added to a saturated solution of acridine, the apparent solubility of acridine increased as a soluble inclusion compound between Acr and βCD was formed. Once the solubility limit of this complex had been reached, any further additions of βCD resulted in the precipitation of a microcrystalline complex due to the low water solubility of the host itself. The A_L-type[9] straight line obtained for the Acr–DMβCD mixture indicated the formation of a soluble 1:1 inclusion complex but the presence of a ternary complex, such as 2:1, could not be excluded. DMβCD contains substituted methyl groups which make it more hydrophobic, and therefore able to complex acridine more effectively. The solubility of acridine at 25 °C is increased by a factor of 2 in 5 mM βCD solution but is increased by a factor of 6 in 5 mM DMβCD solution.

The slope of the solubility curves were also used to deduce the apparent equilibrium constants (K_a) of the inclusion complexes, assuming that the monomer would be the predominant species owing to the very low solubility of acridine in aqueous solution and that the Acr–CD complex has a 1:1 stoichiometry:[9]

$$K_a = \frac{[\text{Acr–CD}]}{[\text{Acr}][\text{CD}]} = \frac{\text{slope}}{(1 - \text{slope})[\text{Acr}]} \qquad (1)$$

where [Acr] is the concentration of free acridine in saturated aqueous solution and [Acr–CD] and [CD] are the concentrations of the complex and of the free cyclodextrin, respectively.

It should be noted that if a series of complexes (Acr–CD, Acr_2–CD, …, Acr_n–CD) were present, an A_L-type system would be observed. However, in the presence of multiple equilibria, the equilibrium constants cannot be deduced directly from solubility data without additional information, and so an apparent binding constant K_a, based on the assumption of 1:1 stoichiometry, is usually used to describe the system.

The measured apparent equilibrium constants K_a were $215 \pm 20\ \text{M}^{-1}$ for Acr–βCD and $1150 \pm 100\ \text{M}^{-1}$ for Acr–DMβCD. For the Acr–βCD complex our result was in reasonable agreement with the value of $287\ \text{M}^{-1}$ deduced from previous fluorescence measurements.[17]

NMR study of acridine in water

Some ambiguity in the interpretation of the NMR data recorded for the Acr–βCD complex led us to check the assignment of the ^{1}H signals of acridine in D_2O solution. Owing to the symmetry of the molecule, only five signals are observed in the ^{1}H spectrum, a singlet at low field (9.16 ppm) assigned to H9, and two doublets (H1 and H4) and two triplets (H2 and H3). In a previous study using DMSO[18] as solvent, it had been shown that H9 is involved in small coupling interactions with H4 and H5 ($^5J = 0.9$ Hz) due to an all-*trans* disposition of the bonds. These are, as expected, greater than ^4J coupling to H1 and H8 (0.5 Hz) with a *cis* disposition of the bonds. The LR-COSY 2D experiment reveals slightly scalar coupled protons. Recorded for acridine in aqueous solution, it

Table 1. ^{1}H NMR chemical shifts, δ (ppm), and coupling constants, J (Hz), of acridine[a]

Atoms	δ (ppm)	Atoms	J (Hz)
H1, H8	8.22	H1–H2	8.4
H2, H7	7.69	H2–H3	6.7
H3, H6	7.95	H3–H4	8.8
H4, H5	8.18	H1–H3	1.3
H9	9.16	H2–H4	1.0
		H1–H4	0.7
		H9–H1	0.5
		H9–H4	0.9

[a] 0.26 mM in D_2O at 298 K.

shows a cross peak at the frequency of H9 (9.16 ppm) and at the frequency of the high-field doublet (8.18 ppm) which then corresponds to H4, H5. This result is inconsistent with the previously reported assignment.[19] In order to confirm our data, an NOE difference experiment was performed. Upon saturating the resonance of H9, a significant response was obtained at 8.22 ppm. The spatial proximity between H9 and the protons at 8.22 ppm leads to the assignment of the low-field doublet to H1, H8. Consequently, the assignment of the high-field doublet to H4, H5 was fully confirmed. Similar experiments were performed in CD_3OD, in which acridine is more soluble than in D_2O. The ^5J coupling was observed between H9 and the doublet at low field (8.19 ppm). Spatial proximity was demonstrated by NOE between H9 and the protons which resonate at high field (8.15 ppm). Hence it clearly appears that, as previously reported,[18] the coupling constants do not change with the solvent, but the relative positions of the protons more proximate to the central ring could obviously be reversed. In all solvents the relative positions of the resonances of H2, H7 and H3, H6 are readily deduced from a COSY experiment and seem to be independent of the solvent. The protons in a *para* position with respect to the nitrogen atom (H2, H7) are the most shielded. The corrected complete assignments are given in Table 1.

NMR study of the Acr–β-cyclodextrin interaction

In order to distinguish the protons of the guest and host molecules, bold characters are used for those of cyclodextrins. The comparison of the spectra recorded before and after adding Acr reveals small differences in the region of the cyclodextrin resonances. The internal protons of the hydrophobic cyclodextrin cavity undergo a slight upfield shift, e.g. **H3** ($\Delta\delta = -0.02$ ppm) and **H5** ($\Delta\delta = -0.03$ ppm) for a solution 0.56 mM in Acr and 5 mM in βCD, whereas the protons of the external face were barely affected. These values are not bound shifts and are therefore lower than values published for bound shifts determined by the use of highly soluble guests.[8] Similarly, comparing the spectrum recorded after adding βCD in an Acr solution with that recorded for the solution of Acr alone in D_2O reveals that the degree to which the protons of acridine are shifted depends on their position with respect to the nitrogen atom. These findings are consistent with an interaction between the two molecules and more precisely with inclusion of the Acr molecule in the cavity of the βCD. Furthermore, the fact that a single signal occurs for each kind of proton at a range of temperatures (5–50 °C) shows that a fast exchange occurs between the free and complexed species. The upfield shifts observed for the protons **H3** and **H5** of the βCD are attributable to anisotropy effects generated by ring currents within the aromatic Acr molecule.

In order to assign unequivocally the signals of acridine protons in the presence of βCD, and to gain more precise information on the interaction between Acr and βCD, the changes in the Acr proton chemical shifts were followed as a function of increasing concentration of βCD. The assignments of the H4, H5 and H1, H8 resonances were obtained after performing an LR-COSY experiment to detect the ^5J coupling interaction of the H4, H5 protons to H9 and a ROESY experiment to demonstrate the spatial proximity of the H1, H8 protons to H9. At 500 MHz the ROESY experiment is appropriate for displaying the proximity of protons in molecules with intermediate molecular weight between 1000 and 1500, whereas the nuclear Overhauser effect could be equal to zero, thus making it impossible to obtain any structural information. The assignment of the other protons is straightforward using coupling interactions (COSY experiment).

As the concentration of βCD was increased, the resonance of H9 was shifted to a greater extent, up to 0.19 ppm to high field. The H1 proton was also significantly shifted up to 0.12 ppm. The resonance of H4 and those of H2 and H3 were only slightly affected (0.05 ppm). It is noteworthy that the shifts for H1 and H4 are in opposite directions, to high field for H1 and to low field for H4. As a result, taking account of their respective positions in the spectrum of pure acridine, the two doublets first converge, until a pseudo-triplet is observed, and then diverge after crossing each other. This finding is inconsistent with the direct divergence postulated in the literature[17,19] (Fig. 4).

Measurement of the binding constant of the Acr–β-CD complex by NMR shift titration

To quantify the complex stability, the binding constant K_a was calculated from the changes in the chemical shifts of the Acr signals recorded as a function of the βCD concentration. The observed chemical shifts δ_{obs} are the weighted average of the chemical shifts for the free δ_f and complexed acridine δ_c under condition of fast exchange.

Assuming a one-to-one binding stoichiometry

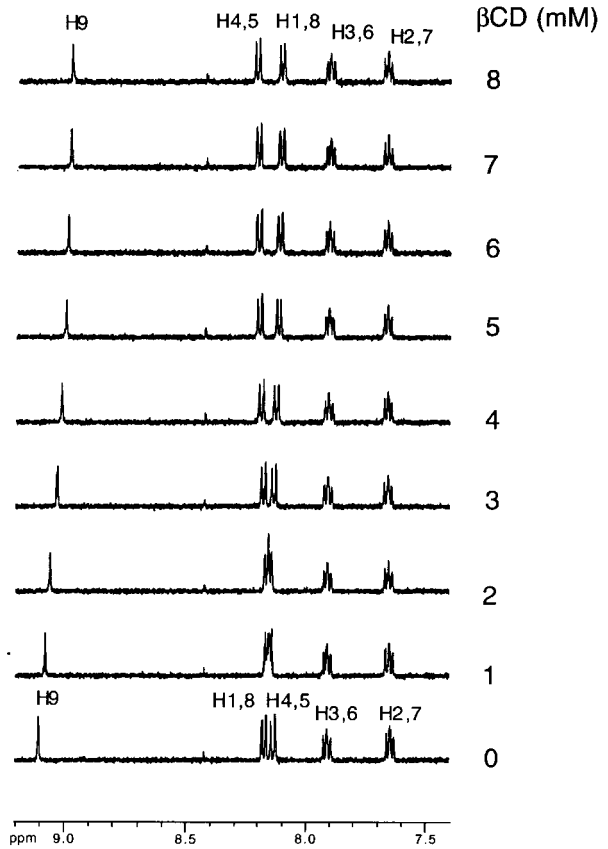

Figure 4. NMR shifts for the titration of acridine (0.2 mM) with βCD in D_2O at 303 K; the signals shift to high field (H9 and H1, H8) and to low field (H4, H5). Signals crossing between (H1, H8) and (H4, H5) is observed during titration

$(A + B \rightleftharpoons AB)$ for the complex [AB], it has been demonstrated that[9]

$$\Delta\delta_{obs} = (\delta_c - \delta_f) \times \frac{([A]_t + [B]_t + K_d) - \sqrt{([A]_t + [B]_t + K_d)^2 - 4[A]_t[B]_t}}{2[A]_t} \quad (2)$$

where $\Delta\delta_{obs} = \delta_{obs} - \delta_f$ for the H9, H4, or H1 protons of Acr in the presence of βCD, $K_a = 1/K_d$, K_a being the binding constant and K_d the dissociation constant, and $[A]_t$ and $[B]_t$ are the total concentrations of Acr and βCD respectively.

Figure 4 shows the change in the ^{1}H spectrum of Acr as a function of the βCD addition. The unknown δ_c and K_a were determined by fitting the experimental values $\Delta\delta_{obs}$ of the Acr H9, H4, and H1 protons to Eqn. (2) using the non-linear least-squares computer program Kaleidagraph (Synergy Software, USA), which uses the Levenberg–Marquardt algorithm. The absence of any systematic deviation and the agreement between the association constants K_a calculated from H9, H4, and H1 data

Table 2. ^{1}H NMR chemical shifts, δ_c (ppm), of (H1, H8), (H4, H5), H9 for the Acr–βCD complex and K_a values obtained from fitting the experimental data to Eqn. (2)

	H1, H8	H4, H5	H9
^{1}H δ_c (ppm)[a]	8.06	8.23	8.93
K_a (M^{-1})	300	323	344

[a] Referenced to DHO at 4.70 ppm, $T = 303$ K.

confirmed the assumed 1:1 stoichiometry. The average equilibrium constant $K_a = 322 \pm 30\ M^{-1}$ (Table 2) was in reasonable agreement with the values of 215 ± 20 and $287\ M^{-1}$, respectively, deduced from the solubility diagrams and from previous fluorescence measurements.[17]

^{1}H spin–lattice relaxation time (T_1) studies

The spin–lattice relaxation times T_1 were measured for acridine in the free state and when complexed with βCD to support the titration experiments. T_1 studies can yield useful information about rapid molecular motions. The T_1 value for any given molecule in solution reflects the overall molecular mobility and specific internal motions determined by internal degree of freedom of the molecule. The correlation time of a guest molecule can usually be obtained from ^{13}C NMR spectra, using longitudinal relaxation T_1 measurements[20] to follow its complexation with the cyclodextrins. The ^{13}C experiments require a high concentration of the guest molecule. The low solubility of acridine in aqueous solution precludes the use of this type of experiment in this study. It has been suggested that a selective null inversion recovery ^{1}H NMR method (SNIDE[15]) could be used to overcome this barrier. The method involves measuring the difference in relaxation rates in a non-selective experiment and in one in which all resonances are inverted except the resonance of the nucleus of interest. This procedure yields cross-relaxation rates between this nucleus and all other nuclei in dipolar interaction. These rates can be used to determine the motional correlation time τ_{ij} for the reorientation of the internuclear vector involved. The method can be used for both free and complexed acridine to provide evidence of any change in dynamics as a result of the binding process.

In a multi-spin system, the longitudinal relaxation rate of a given spin i can be approximated as

$$R_1^i(\text{ns}) = \frac{1}{T_1^i(\text{ns})} = \sum_{j \neq i} \rho_{ij} + \sum_{j \neq i} \sigma_{ij} + \rho^* \quad (3)$$

where ns relates to non-selective inversion experiment, ρ_{ij} is the longitudinal dipolar relaxation rate constant of proton i due to dipolar interaction with proton j, $\sigma_{ij}(\sim\sigma_{ji})$

is the cross relaxation rate constant between proton i and j, ρ^* covers all non-dipolar relaxation terms.

Using the null inversion sequence with, e.g., the spin k not inverted, the relaxation rates of the protons are

$$R_1^i(k \text{ not inverted}) = \sum_{j \neq i} \rho_{ij} + \sum_{j \neq k} \sigma_{ij} + \rho^* \quad (4)$$

The cross-relaxation term between nucleus i and nucleus k is then

$$\sigma_{ik} = R_1^i(\text{ns}) - R_1^i(k \text{ not inverted}) \quad (5)$$

It is noteworthy that all contributions to non-dipolar relaxation are canceled in the difference.

It has been shown that the derived relaxation rates, σ_{ij}, can be approximately related to the internuclear distance, r_{ij}, and to the motional correlation time, τ_{ij}, for reorientation of the involved internuclear vector by the relation

$$\sigma_{ij} = \frac{\hbar^2 \gamma_H^4}{10 r_{ij}^6} \tau_{ij} \left(\frac{6}{1 + 4\omega^2 \tau_{ij}^2} - 1 \right) \quad (6)$$

where $\hbar$ is the reduced Planck's constant, γ_H is the proton gyromagnetic ratio and $\omega = \omega_i \approx \omega_j$ is the Larmor precession frequency of proton. τ_{ij} can then be calculated knowing the internuclear distance r_{ij} for each pair of protons.

For free acridine, reorientation motions occur within the extreme narrowing region such that $\omega\tau_{ij} \ll 1.12$ and positive values of σ_{ij}^f are observed. In this case Eqn. (6) simplifies to

$$\sigma_{ij}^f = \frac{\hbar^2 \gamma_H^4}{2 r_{ij}^6} \tau_{ij}^f \quad (7)$$

It should be noted that the correlation time of one internuclear vector can be markedly different from that of another owing to the anisotropy of the reorientation motion.

Under conditions where acridine is in rapid equilibrium between a free state and a complexed state, and assuming one-to-one binding stoichiometry, the measured cross-relaxation rate (σ_{ij}^{obs}) will be a weighted average of the cross-relaxation rates for the free (σ_{ij}^f) and the complexed (σ_{ij}^c) acridine (x is the molar fraction of free acridine):

$$\sigma_{ij}^{obs} = x\sigma_{ij}^f + (1 - x)\sigma_{ij}^c \quad (8)$$

The slower motion of the complexed acridine, in contrast, results in $\omega\tau_{ij} \geq 1.12$. As a consequence, a null value for σ_{ij}^{obs} might be reached for the appropriate value $1–x$ of the fraction of bound acridine. Under these conditions, knowledge of x (via K_a and $[A]_t$) makes it possible to calculate the σ_{ij}^c rate in the bound state [Eqn. (8)] and then to determine the motional correlation time τ_{ij}^c of the H_i–H_j vector by solving the equation

$$\tau_{ij}^c \left(\frac{6}{1 + 4\omega^2 \tau_{cij}^2} - 1 \right) = \frac{5x}{x - 1} \tau_{ij}^f \quad (9)$$

^{1}H NMR SNIDE experiments were performed on a 0.26 mM solution of acridine in D_2O. Six experiments are sufficient to obtain all relaxation rates five using null inversion and one non-selective inversion–recovery. The relaxation rates derived are summarized in Table 3 together with the non-selective relaxation rates. The relaxation rate differences [σ_{ij}^f, Eqn. (5)] between relevant dipolar relaxation rates and the ^1H_i–^1H_j internuclear distances r_{ij} are directly related to the molecular correlation time τ_{ij}^f through Eqn. (7). The results are averages of three independent determinations obtained at 303 K: $\tau_{1,9}^f = 2.3 \times 10^{-11}$ s (from $\sigma_{1,9}$, $\sigma_{9,1}$ and $r_{1,9} = 2.484$ Å), $\tau_{1,2}^f = 1.6 \times 10^{-11}$ s (from $\sigma_{2,1}$, $\sigma_{1,2}$ and $r_{1,2} = 2.473$ Å), $\tau_{2,3}^f = 1.3 \times 10^{-11}$ s (from $\sigma_{2,3}$, $\sigma_{3,2}$ and $r_{2,3} = 2.483$ Å) and $\tau_{3,4}^f = 1.8 \times 10^{-11}$ s (from $\sigma_{3,4}$, $\sigma_{4,3}$ and $r_{3,4} = 2.485$ Å). The differences observed between the correlation times of H9–H1, H3–H2, H3–H4 and H2–H1 internuclear vectors have been attributed to the anisotropic reorientation of the free acridine which can be approximated to an ellipsoid. This hypothesis was confirmed by ^{13}C NMR relaxation time measurements and derived correlation times for acridine in methanol.

In order to gain some information about the acridine–cyclodextrin interaction, the SNIDE method was repeated

Table 3. 500 MHz ^{1}H NMR non-selective and selective inversion relaxation rates R_1 (s^{-1})[a] for 0.26 mM acridine in D_2O[b]

	H1, H8	H2, H7	H3, H6	H4, H5	H9
^{1}H δ (ppm)[c]	8.17	7.65	7.91	8.14	9.10
R_1: non-selective	0.244	0.207	0.213	0.165	0.277
R_1: H1, H4 not inverted	—	0.184	0.193	—	0.212
R_1: H2 not inverted	0.226	—	0.198	0.167	0.285
R_1: H3 not inverted	0.252	0.189	—	0.142	0.281
R_1: H9 not inverted	0.223	0.208	0.214	0.166	—

[a] All relaxation rates were calculated using the standard three-parameter method; standard deviation of R_1 is 3%.
[b] Non-deoxygenated solution, $T = 303$ K.
[c] Referenced to 4.70 ppm DHO.

Table 4. 500 MHz ^{1}H NMR non-selective and selective inversion relaxation rates R_1 (s^{-1})[a] for the protons of 0.56 mM acridine in the presence of 5 mM βCD in D_2O; $T = 303$ K

	H1, H8	H2, H7	H3, H6	H4, H5	H9
^{1}H δ (ppm)[b]	8.07	7.60	7.86	8.17	8.93
R_1: non-selective	0.659	0.492	0.528	0.512	0.750
R_1: H1, H8 not inverted	—	0.482	0.535	0.523	0.754
R_1: H2, H7 not inverted	0.648	—	0.527	0.521	0.762
R_1: H3, H6 not inverted	0.669	0.496	—	0.507	0.762
R_1: H4, H5 not inverted	0.680	0.499	0.522	—	0.755
R_1: H9 not inverted	0.656	0.495	0.528	0.517	—

[a] All relaxation rates were calculated using the standard three-parameters method; standard deviation of R_1 is 3%.
[b] Referenced to 4.70 ppm DHO.

using saturated acridine solutions in the presence of 5 mM βCD. The viscosity of aqueous cyclodextrin solutions is only insignificantly different from that of water.[21]

The data obtained in the presence of the cyclodextrin are summarized in Table 4. ^{1}H T_1(ns) measured for acridine hydrogen showed an average reduction of 40% when βCD was added. This confirms that acridine did indeed complex with the cyclodextrin. As a consequence of negative σ_{ij}^{c} values for complexed acridine, the difference between null selective rates and non-selective rates provided a null value of σ_{ij}^{obs} for all ^1H_i–^1H_j proton pairs, taking into account the standard deviation, which was $\leq$3%. The occurrence of motion close to the limit of the extreme narrowing region was also confirmed by measuring a null NOE value in NOE 1D, and by the absence of cross-correlation peaks in NOESY 2D experiments.

Knowing the binding constant for the system Acr–βCD, 322 M^{-1}, it can be calculated that the concentration of the pure complex is 0.34 mM. Then the correlation time τ_{ij}^{c} for complexed acridine are calculated by solving Eqn. (9).

The values obtained are for the Acr–βCD system: $\tau_{1,9}^{c} = 3.9 \times 10^{-10}$ s, $\tau_{1,2}^{c} = 3.7 \times 10^{-10}$ s, $\tau_{2,3}^{c} = 3.7 \times 10^{-10}$ s and $\tau_{3,4}^{c} = 3.9 \times 10^{-10}$ s. When acridine was included in cyclodextrin, its overall tumbling motion was significantly slowed. The homogeneous values of τ_{ij}^{c} derived for the reorientation of all internuclear H_i–H_j vectors showed that acridine undergoes a nearly isotropic reorientation in pure complexes. The average correlation time of the complexed acridine, $\tau^{c} = 3.8 \times 10^{-10}$ s, is very similar to that of the βCD, suggesting that acridine motion is dynamically strongly coupled to that of the CD. Acridine is no longer free to rotate and its motional correlation time is determined by that of the cyclodextrin molecule. Assuming a spherical model[22] and taking into account the viscosity of the solvent (0.798 Cp) at 303 K, the Acr–βCD complex appears to behave in solution as a sphere with a diameter around 15 Å.

The form of the acridine molecule can be approximated to an axially symmetric ellipsoid in which the principal axis nearly bisects the C2—C3 and C6—C7 bonds and a secondary axis coincides with the N—H9 direction. Given the size of acridine (approximately 9×5 Å) and of the βCD cavity (7.8 Å), it is clear that βCD could accommodate a large part of the acridine molecule in its cavity, provided that the insertion occurs along the principal axis of the ellipsoid. Owing to the rapidity of the exchange between the free and complexed molecule and to the symmetry of the acridine molecule, which precludes either ring A or ring C being favored, the pairs of protons which are chemically equivalent in free acridine are not distinguished.

A ROESY experiment is suitable for obtaining information about the spatial proximity between atoms of the host and guest molecules by observing the intermolecular dipolar cross-correlations. The intensities of the cross peaks are proportional to $1/r^6$, where r represents the mean distance between the protons in dipolar interaction. From a semi-quantitative point of view, it could be expected that the H9 proton, in the middle part of Acr, which is always included in the cavity, gives intense correlations with the internal **H3**, **H5** protons of βCD. The experimental data (Fig. 5) agree well with this hypothesis. It is worth noting that the intensities of corresponding cross peaks are very similar. The A/C rings switch between two positions, one inside the cavity, at the top, and other at the bottom or even outside the cavity. The cross peak intensities between the A/C ring protons and the internal **H3**, **H5** βCD protons could be expected to be different. For all the acridine protons the correlations are more intense with **H5** situated in the upper part of the cavity than for **H3**, the difference being far greater for the interactions involving the H2, H7 and H3, H6 than for those involving H4, H5 and H1, H8 which are in a more central position in the acridine molecule. Finally, the correlations of **H5** and also those of **H3** were found to be more intense with H4, H5 and H3, H6 than with H1, H8 and H2, H7. This observation suggests the displacement of the principal axis of acridine relative to the symmetry axis of βCD such that H4, H5 and H3, H6 are located nearer to the wall of the internal cavity than H1, H8 and H2, H7. The lack of any cross peak between the Acr protons and either **H2** or **H4**, external protons of βCD, precludes significant non inclusion interactions between Acr and βCD.

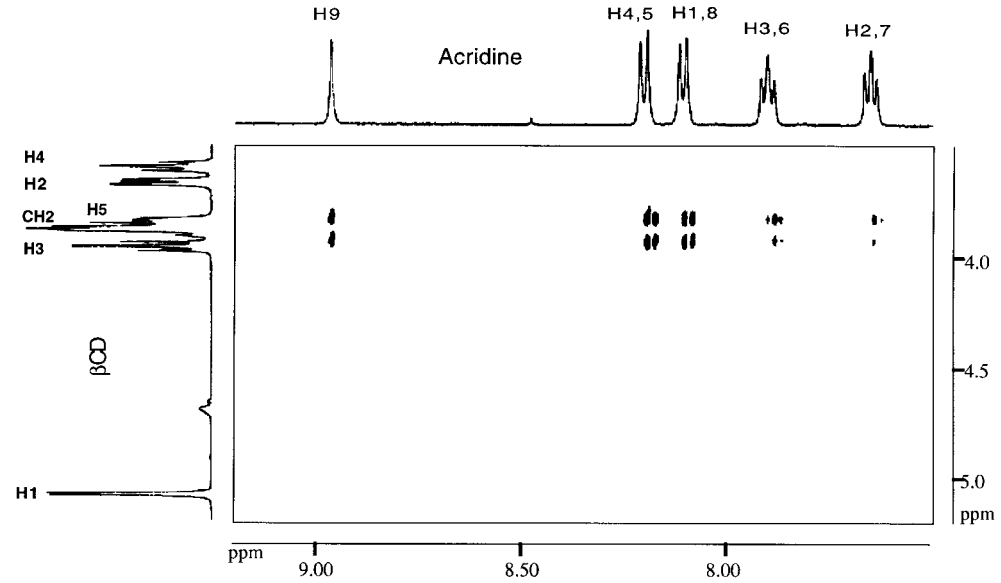

Figure 5. Partial contour plot of a ROESY off-resonance adiabatic experiment performed on the acridine–βCD mixture showing dipolar interactions between the protons of acridine and cyclodextrin (500.11 MHz, 310 K)

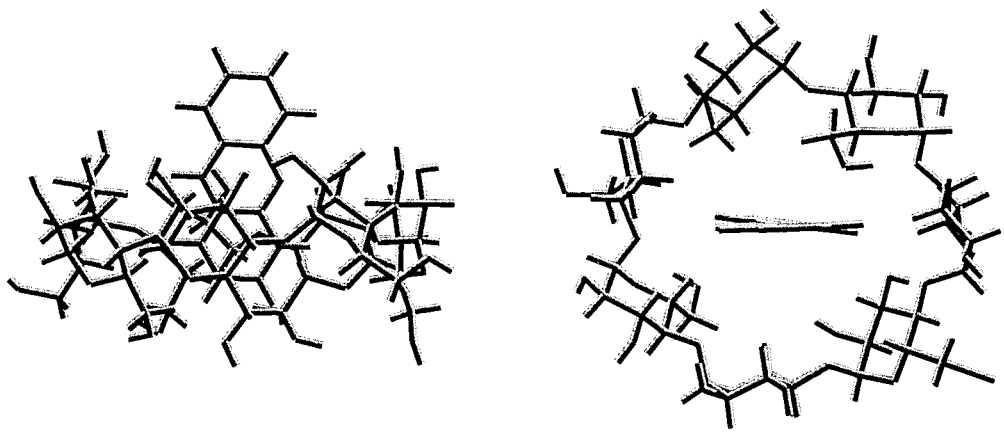

Figure 6. 3D molecular models of acridine–βCD complex derived from 2D ROESY data

Molecular modeling

Molecular and dynamic modeling with NMR intermolecular constraints was used to position the acridine in the βCD cavity. ROE constraints were introduced between the acridine protons of rings A and B (H1, H2, H3, H4 and H9) and the **H3** and **H5** protons of the cyclodextrin. The twenty most energetically stable structures were superimposed to achieve the best fit of the backbone atoms. Figure 6 shows one of the molecular models of the Acr–βCD complex where the acridine molecule is half inserted into the internal hydrophobic cavity of the βCD, that corresponds to the most stable conformation. Electrostatic repulsive forces between internal protons of the cavity and protons of the ligand prevent the ligand from crossing the cyclodextrin. The position of acridine is stabilized by hydrophobic interactions between the protons of A ring and H9 with the **H3**, **H5** protons of the internal cyclodextrin cavity, a hydrogen bond between the nitrogen atom of acridine with one C3—OH of βCD.[19] The structure of the complex was consistent with the NMR results and confirmed the inclusion model. The acridine molecule is partly inserted into the βCD cavity along its ellipsoid axis by all of the A and half of the B ring.

NMR study of the acridine–heptakis(2,6-di-*O*-methyl)-β-cyclodextrin interaction

In heptakis(2,6-di-*O*-methyl)-β-cyclodextrin (DMβCD), each of the glucopyranoside rings has two methoxy groups at positions 2 and 6. In order to determine the shifts of all ^{1}H and ^{13}C resonances of DMβCD in D_2O, 1D spectra and a series of 2D experiments were

Table 5. ^{1}H NMR (800 MHz) and ^{13}C NMR (125 MHz) chemical shifts, δ (ppm), and coupling constants, J_{H-H} (Hz), of DMβCD (5 mM in D_2O) at 303 K

	C1–H1	C2–H2	C3–H3	C4–H4	C5–H5	C6–H6	2-OCH_3	6-OCH_3
δ ^{1}H (ppm)	5.22	3.35	3.94	3.58	3.87	3.73(6)–3.69(6)	3.53	3.37
δ ^{13}C (ppm)	99.34	81.73	72.32	82.28	70.33	70.93	59.53	58.64
	H1–H2	H2–H3	H3–H4	H4–H5	H5–H6	H5–H6	H6–H6	
J (Hz)	3.6	10.1	9.5	9.5	4.6	1.5	−11.4	

performed at 303 K. Homonuclear and heteronuclear correlations (COSY, HSQC and HMBC) made it easy to assign all the signals except those of the methoxy groups. The results obtained are in good agreement with those previously reported.[23] The assignments were completed by an HMBC experiment which was used to demonstrate ^3J correlations between C2, C6 and the protons of the corresponding attached OCH_3 groups. It is noteworthy that correlations were also observed within the ring carbons and the attached protons, C3 and C5 with H1 (^3J), C2 with H3 (^2J). The results are given in Table 5.

The interaction between Acr and DMβCD was studied in the same way as for the Acr–βCD complex. A 1D ^{1}H spectrum was recorded for a solution of acridine and DMβCD in which the total concentration of acridine determined by UV spectrophotometry was found to be 1.4 mM. The comparison of this spectrum with those recorded for a solution of pure DMβCD and for a solution of Acr alone led to the same qualitative conclusions as for βCD. Complexation involved the inclusion of Acr in DMβCD, and a fast exchange occurred between free and complexed species. In agreement with a higher value of the apparent binding constant, K_a, deduced from the solubility diagram, the effects observed in the NMR spectra were more intense than for βCD, e.g. upfield shifts for **H3** (0.07 ppm) and **H5** (0.08 ppm) of DMβCD and upfield shifts for H9 (0.47 ppm), and H2 and H3 (0.13 ppm) of acridine (for a solution 1.40 mM in Acr and 5 mM in DMβCD). Finally, the H1 and H4 protons both moved to high field, but once again the signals crossed each other. The shielding effect of complexation on H1, which was initially slightly less shielded than H4, was far stronger than for H4. In contrast to βCD, the titration curves obtained with DMβCD were not representative of a 1:1 stoichiometry. Non-linear least-squares fitting of the H9, H1 and H4 shifts yielded individual apparent K_a values differing by more than 10% and fitting to a 1:1 model revealed systematic deviations. This calls for the investigation of additional equilibria. The Acr–DMβCD system has been analyzed on the basis of the assumption that 1:1 and 2:1 adducts are present under the condition of fast exchange. It was assumed that each complex is formed in a bimolecular process: (i) inclusion of one acridine molecule and then (ii) interaction with a second guest molecule. Consequently, the two inclusion complexes could be related by the following equilibria:

$$\text{Acr} + \text{DM}\beta\text{CD} \rightleftharpoons \text{Acr–DM}\beta\text{CD} \qquad K_{1:1}$$

$$\text{Acr} + \text{Acr–DM}\beta\text{CD} \rightleftharpoons \text{Acr}_2\text{–DM}\beta\text{CD} \qquad K_{2:1}$$

characterized by the stepwise binding constants.

$$K_{1:1} = \frac{[\text{Acr–DM}\beta\text{CD}]}{[\text{Acr}][\text{DM}\beta\text{CD}]} \tag{10}$$

$$K_{2:1} = \frac{[\text{Acr}_2\text{–DM}\beta\text{CD}]}{[\text{Acr}][\text{Acr–DM}\beta\text{CD}]} \tag{11}$$

where [Acr], [DMβCD], [Acr–DMβCD] and [Acr_2–DMβCD] are the equilibrium molar concentration of species present in solution. The weighted average expression for the observed chemical shifts of the protons of acridine is

$$\delta_{obs} = \frac{[\text{Acr}]}{[\text{Acr}]_t}\delta_f + \frac{[\text{Acr–DM}\beta\text{CD}]}{[\text{Acr}]_t}\delta_{\text{Acr–DM}\beta\text{CD}} + 2\frac{[\text{Acr}_2\text{–DM}\beta\text{CD}]}{[\text{Acr}]_t}\delta_{\text{Acr}_2\text{–DM}\beta\text{CD}} \tag{12}$$

where $[Acr]_t$ is the global concentration of acridine and δ_f, $\delta_{Acr-\beta CD}$ and $\delta_{Acr_2-DM\beta CD}$ are the chemical shifts of the same proton signals for the free acridine and for the binary and ternary complexes respectively.

The changes in the chemical shifts of the guest molecule signals as a function of host concentration added were analyzed by curve fitting software using a 2:1 complexation (bimolar process) model described in literature[24] (the *NMRTit* program was available from Hunter *et al.*[24] on request). The theoretical curves obtained yielded $K_{1:1} = 575 \pm 60\ M^{-1}$ and $K_{2:1} = 550 \pm 60\ M^{-1}$. The chemical shifts for the H1, H4 and H9 protons of acridine complexed with DMβCD are summarized in Table 6. The equations that were obtained required fitting with four variables for each proton of acridine, and thus many solutions can satisfy the model.

Table 6. ^{1}H NMR chemical shifts, δ_c (ppm), of (H1,H8), (H4,H5), H9 for the Acr–DMβCD complexes and K_a values obtained from fitting the experimental data with the *NMRTit* program[24]

	H1, H8	H4, H5	H9
^{1}H $\delta_{Acr-DM\beta CD}$ ppm[a]	8.07	8.26	8.83
^{1}H $\delta_{Acr_2-DM\beta CD}$ ppm[a]	7.71	6.18	7.52
$K_{1:1}$ (M^{-1})	535	540	652
$K_{2:1}$ (M^{-1})	522	543	583

[a] Referenced to DHO at 4.70 ppm, $T = 303$ K.

Consequently, the values obtained should be regarded as indicating trends rather than actual values.

The effects of complexation on acridine motion were studied by means of T_1 measurements. The SNIDE experiment was performed using a 1.4 mM solution of acridine in D_2O in presence of 5 mM DMβCD. The relaxation rates measured for the mixture are given in Table 7. The non-selective cross-relaxation rates of acridine protons increased when DMβCD was added as a result of a complexation. The changes in the acridine R_1 (ns) values were greater in the presence of DMβCD than with βCD. This suggests that acridine binds most strongly to DMβCD. This observation is consistent with solubility diagrams measurements. The occurrence of motion outside the narrowing region was verified by a null value of $\sigma_{i,j}^{obs}$ observed for all proton pairs of complexed acridine in dipolar interaction. Knowing the apparent equilibrium constant, $K_a = 1150\ M^{-1}$, determined by the solubility diagrams method and assuming a 1:1 system for Acr–DMβCD, a rough estimate of the pure complex concentration, 1.14 mM, is obtained. The estimated values of the correlation times, $\tau^c_{i,j}$, for Acr–DMβCD are then $\tau^c_{1,9} = 3.7 \times 10^{-10}$ s, $\tau^c_{1,2} = 3.6 \times 10^{-10}$ s, $\tau^c_{2,3} = 3.7 \times 10^{-10}$ s and $\tau^c_{3,4} = 3.9 \times 10^{-10}$ s. The average correlation time of the complexed acridine, $\tau^c = 3.7 \times 10^{-10}$ s, suggests that the motion is strongly coupled to that of DMβCD. Finally, significant differences were observed in the ROESY experiments recorded for acridine complexed by either of the cyclodextrins. In contrast to the findings with βCD, the cross peaks corresponding to the dipolar interactions involving the internal protons of DMβCD, **H3** and **H5**, with all the protons in rings A, and C of acridine had strong similar intensities (Fig. 7). New interactions occurred between all the protons of acridine and those of the C2- and C6-methoxy groups. The cross peaks had relatively low intensity with regard to the C2—O**C**$\mathbf{H}_3$ group but had strong intensity with regard to the C6—CH_2OC$\mathbf{H}_3$ group. One medium intensity correlation was observed between the 6-C$\mathbf{H}_2$ group and the lone H4 proton in acridine. Above all, these findings confirmed the inclusion of an acridine molecule. This was partially hampered by the formation of a hydrophobic plug at the top of the host molecule, due to the presence of the C6—CH_2OCH_3 groups, but probably most firmly maintained by a supplementary interaction with the C2—OCH_3 groups at the bottom of the cavity. Furthermore, the strong dipolar correlations between all the acridine protons and the C6—CH_2OC$\mathbf{H}_3$ groups were only compatible with interaction between DMβCD and an acridine molecule which remains outside the cavity and proximate to the plug formed by the primary hydroxyl groups at the top of the CD ring.

CONCLUSION

A combination of the solubility diagrams method and ^{1}H NMR spectroscopy was used to demonstrate complexation between the cyclodextrins βCD and DMβCD and acridine. The findings of the solubility diagrams study indicate that both βCD and DMβCD increase the apparent water solubility of acridine. The increase in solubility was greater for DMβCD than for βCD. The B_s-type curve of the aqueous concentration of acridine versus the concentration of βCD suggests a 1:1 complex with low solubility ($K_a = 215 \pm 20\ M^{-1}$), whereas the A_L-type curve obtained for the Acr–DMβCD system indicates a more soluble complex ($K_a = 1150 \pm 100\ M^{-1}$), possibly with different stoichiometries (1:1 and/or 2:1, etc.). The complexes between acridine and βCD or DMβCD were characterized by NMR changes in

Table 7. 500 MHz ^{1}H NMR non-selective and selective inversion relaxation rates R_1 (s^{-1})[a] for protons of 1.40 mM acridine in the presence of 5 mM DMβCD in D_2O, $T = 303$ K

	H1, H8	H2, H7	H3, H6	H4, H5	H9
^{1}H δ(ppm)[b]	7.96	7.55	7.81	8.13	8.69
R_1: non-selective	0.79	0.68	0.66	0.70	0.83
R_1: H1, H8 not inverted	—	0.67	0.66	0.69	0.75
R_1: H2, H7 not inverted	0.78	—	0.68	0.71	0.89
R_1: H3, H6 not inverted	0.70	0.69	—	0.70	0.84
R_1: H4, H5 not inverted	0.76	0.68	0.65	—	0.81
R_1: H9 not inverted	0.82	0.66	0.65	0.69	—

[a] All relaxation rates were calculated using the standard three-parameters method; standard deviation of R_1 is 3%.
[b] Referenced to 4.70 ppm DHO.

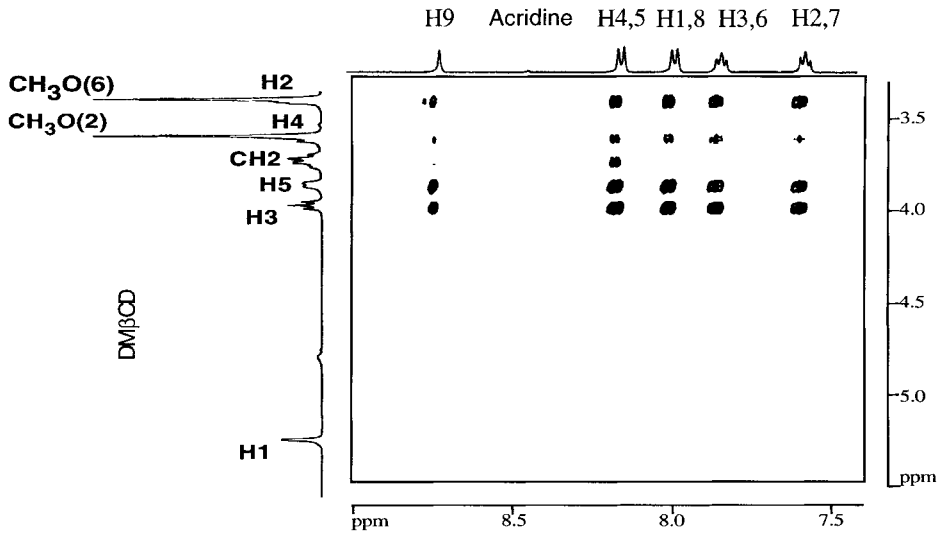

Figure 7. Partial contour plot of a ROESY off-resonance adiabatic experiment performed on the acridine–DMβCD mixture showing dipolar interactions between the protons of acridine and cyclodextrin (500.11 MHz, 303 K)

the chemical shifts of some of the acridine protons as a function of CD concentration. The chemical shifts in the signals of acridine protons when it was complexed gave an association constant of $322 \pm 30\ \text{M}^{-1}$, assuming 1:1 stoichiometry for the Acr–βCD system, and stepwise binding constants of $K_{1:1} = 575 \pm 60\ \text{M}^{-1}$ and $K_{2:1} = 550 \pm 60\ \text{M}^{-1}$ for 1:1 and 2:1 stoichiometries, respectively, for the Acr–DMβCD mixture. We also used ^{1}H T_1 measurements to provide information on the motional freedom of acridin when it was bound to cyclodextrins. Both inclusion complexes were of the 'strongly coupled' type from the dynamic point of view, i.e. the motions of acridine were the same as those of cyclodextrins involved in the complexation. Although the approach described here is limited to guest molecules that contain at least a pair of protons with a fixed internuclear distance, it has been shown to be a suitable method for examining complexation of guests under conditions where complexation-induced shifts are small and the concentration of the sample is low. A combination of experimental ROE values and MD simulations allowed us to study the geometry of the inclusion complexes of acridine. Our findings indicate the following: (i) the acridine molecule can be approximated by an ellipsoid which is partially inserted along its principal axis into the βCD cavity, (ii) in the Acr–DMβCD complex one molecule of acridine seems to penetrate the cavity of cyclodextrin more deeply from the secondary side, and a second molecule may also interact with the DMβCD on the OCH_3 primary side, but it remains outside the cavity. This may be the most likely explanation for the significantly higher affinity constant of acridine towards DMβCD than βCD. Consequently, the use of DMβCD as a means of increasing the water solubility of acridine could improve the bioavailability of the potential cholinesterase inhibitor Acr-$COO(CH_2)_n$ $C_5H_5N^+Cl^-$.

Supplementary material

The supplementary material available at the epoc website at http://www.wiley.com/epoc contains the following: ^{1}H (800 MHz) and ^{13}C (125 MHz) NMR spectra of DMβCD; curve fitting of $\Delta\delta_{obs}$ for H9, H4, and H1 Acr NMR signals recorded as a function of the βCD and of the DMβCD concentration [non-linear least-squares computer program: Kaleidagraph program (Synergy Software, USA) with the Levenberg–Marquardt algorithm]; and an example of the selective relaxation rate measurement of Acr protons by the selective null inversion–recovery pulse sequence.

REFERENCES

1. (a) Le Texier L, Favre E, Redeuilh C, Blavet N, Bellahsene T, Dive G, Pirotzky E, Godfroid JJ. *J. Lipid Mediators Cell Signalling* 1996; **13**: 189–205; (b) Le Texier L, Favre E, Ronzani N, Massicot F, Blavet N, Pirotzky E, Godfroid JJ. *J. Lipid Mediators Cell Signalling* 1996; **13**: 207–222.
2. Ronzani N. *Analusis* 1995; **23**: 164–168.
3. Acheson RM. *Acridines* (2nd edn). Interscience: New York, 1973; chapt. 9.
4. Uekama K, Hirayama F, Irie T. *Chem. Rev.* 1998; **98**: 2045–2076.
5. (a) Duchêne D (ed). *Cyclodextrins and Their Industrial Uses*. Editions de Santé: Paris, 1987; (b) Szejtli J. *Cyclodextrin Technology*. Kluwer: Dordrecht, 1988; (c) Uekama K. *Yakugaku Zasshi* 1981; **101**: 857; (d) Szejtli J, Osa T. *Comprehensive Supramolecular Chemistry*. Vol. 3: Cyclodextrins. Elsevier: Oxford, 1996; (e) Szejtli J. *J. Inclusion Phenom.* 1983, **1**, 135; (f) Djedaini F, Perly B. *J. Pharm. Sci.* 1991; **80**: 1157–1161.
6. Hedges AR. *Chem. Rev.* 1998; **98**: 2035–2044, and references cited therein.
7. (a) Szejtli J. *Cyclodextrins and Their Inclusion Complexes*. Akadémiai Kiadó: Budapest, 1982; (b) Uekama K. *Pharm. Int.* 1985; **6**, 61; (c) Uekama K, Otagiri M. *CRC Crit. Rev. Ther. Drug Carrier Syst.* 1987; **3**: 1; (d) *Drugs Future* 1984; **9**: No. 8.
8. Schneider HJ, Hacket F, Rüdiger V, Ikeda H. *Chem. Rev.* 1998; **98**: 1755–1786, and references cited therein.
9. (a) Higuchi T, Connors KA. *Adv. Anal. Chem. Instrum.* 1965; **4**:

117–212; (b) Connors KA. *Binding Constants: the Measurement of Molecular Complex Stability*. Wiley: New York, 1987; chapt. 5.
10. Derome AE. *Modern NMR Techniques for Chemistry Research*. Pergamon Press: Oxford, 1991; 183–234.
11. Schleucher J, Schwendinger M, Griesinger C. *J. Biomol. NMR* 1994; **4**: 301–306.
12. Wilker W, Leibfritz D, Kesserbaum R, Bermel W. *Magn. Reson. Chem.* 1993; **31**: 287–292.
13. Bothner-By AA, Stephens RL, Lee J, Warren CD, Jeanloz RW. *J. Am. Chem. Soc.* 1984; **106**: 811–813.
14. (a) Desvaux H, Berthault P, Birlirakis N, Goldman M. *J. Magn. Reson. A* 1993; **108**, 219; (b) Desvaux H, Berthault P, Birlirakis N, Goldman M, Piotto M. *J. Magn. Reson. A* 1995; **113**: 47–52.
15. Liu M, Lindon JC. *Concepts Magn. Reson.* 1996; **8**: 161–173.
16. Ivanov PM, Salvatierra D, Jaime C. *J. Org. Chem.* 1996; **61**: 7012–7017.
17. Schuette JM, Ndou T, Muñoz de la Peña A, Greene KL, Williamson CK, Warner IM. *J. Phys. Chem.* 1991; **95**: 4897–4902.
18. Angerman NS, Danyluk SS. *Org. Magn. Reson.* 1972; **4**: 895–906.
19. (a) Schuette JM, Ndou T, Muñoz de la Peña A, Mukundan S Jr, Warner IM. *J. Am. Chem. Soc.* 1993; **115**: 292–298; (b) Schuette JM, Warner IM. *Anal. Lett.* 1994; **27**: 1175–1182.
20. Behr JP, Lehn JM. *J. Am. Chem. Soc.* 1976; **98**: 1743–1747.
21. Flohr K, Paton RM, Kaiser ET. *J. Am. Chem. Soc.* 1975; **97**: 1209–1218.
22. Abragam A. *The Principles of Nuclear Magnetism*. Oxford University Press: London, 1961.
23. Yamamoto Y, Onda M, Takahashi Y, Inoue Y, Chujo R. *Carbohydr. Res.* 1987; **170**: 229–234.
24. Bisson AP, Hunter CA, Morales JC. Young K. *Chem. Eur. J.* 1998; **4**: 845–851.

